ISBN: 978-3-95450-220-2 ISSN: 2673-5474 doi: 10.18429/JACoW-FEL2022-TUP10

EXPERIMENTAL DEMONSTRATION OF TEMPORALLY SHAPED PICOSECOND OPTICAL PULSES FOR DRIVING ELECTRON PHOTOINJECTORS

R. Lemons *, N. Neveu, J. Duris, A. Marinelli, C. Durfee, S. Carbajo

SLAC National Accelerator Laboratory, 2575 Sand Hill Rd, Menlo Park CA, 94061, USA
Colorado School of Mines, 1500 Illinois St, Golden CO, 80401, USA
University of California, Los Angeles, 420 Westwood Plaza, Los Angeles, CA 90095

Abstract

Next-generation electron photoinjector accelerators, such as the LCLS-II photoinjector, have increasingly tight requirements on the excitation lasers, often calling for tens of picosecond, temporally flat-top, ultraviolet (UV) pulse trains to be delivered at up to 1 MHz. We present an experimental demonstration of temporal pulse shaping for the LCLS-II photoinjector laser resulting in temporally flat-top pulses with 24 ps durations. Our technique is a non-colinear sum frequency generation scheme wherein two identical infrared optical pulses are imparted with equal and opposite amounts of spectral dispersion. The mixing of these dispersed pulses within a thick nonlinear crystal generates a second harmonic optical pulse that is spectrally narrowband with a designed temporal profile [1]. In the experiment, we achieve upwards of 40% conversion efficiency with this process allowing this to be used for high average and peak power applications. These narrowband pulses can then be directly upconverted to the UV for use in driving free electron laser photocathodes. Additionally, we present a theoretical framework for adapting this method to shape optical pulses driving other photoinjector-based applications.

INTRODUCTION

In photoinjectors, electrons are generated via the photoelectric effect with laser pulses comprised of light above the work function of the material. During emission, the temporal intensity profile of the laser pulse can significantly affect electron bunch quality. A key measure of quality is the transverse emittance, ϵ_x, defined as [2]

$$\epsilon_x = \sqrt{\langle x_i^2 \rangle \langle x_i'^2 \rangle - \langle x_i^2 x_i'^2 \rangle} \tag{1}$$

where x is the transverse position and x' is the corresponding angle with respect to the ideal trajectory. For generation of x-rays from x-ray free electron lasers (XFELs), it is critical to have electron bunches that are generated with low emittance ($< 1.5\ \mu$m), narrow energy spread ($\Delta E/E < 10^{-3}$), and good spatial uniformity [3]. The latter two quantities can be improved to some extent after generation through the use of spatio-temporally shaped IR lasers in laser heaters [4–6], however initial transverse emittance is dominantly controlled through the temporal intensity profile of the excitation laser pulse. Conventionally implemented photoexcitation laser profiles are Gaussian in time though other commonly sought-after laser distributions are shown to reduce transverse emittance such as flat-top spatiotemporal profiles resembling cylinders [7] or 3D ellipsoids such that the beam size and intensity vary as a function of time [8].

Producing excitation laser pulses with non-Gaussian temporal intensity profiles and duration on the order of 10s of picoseconds is non-trivial. Pulses of the temporal duration lack the spectral content for shaping methods such as spatial-light modulators [9] or acousto-optic modulators [10] to be effective and are shorter than the response time for direct temporal electro-optic modulators [11]. Additionally, the high-repetition rate and pulse energy requirements of next-generation XFELs such as LCLS-II [12] approaches or exceeds the material damage threshold for these devices [13] further complicating their use for shaping the excitation laser pulses. One method that has seen promise for pulse shaping for XFEL facilities is pulse stacking [14] where multiple copies of a short pulse are coherently added in time to generate the desired composite intensity profile. However, pulses generated with the method have been shown to induce unwanted microbunching [15, 16] on the electron bunch resulting in increased emittance relative to Gaussian distributions. Furthermore, the series of nonlinear conversion stages to upconvert infrared (IR) light to UV light below 270 nm [17, 18] present in all XFEL photo-excitation laser systems is detrimentally affected by non-zero phase structure on the pulses, distorting temporal profiles, complicating shaping efforts, and limiting the applicability to high average power, 24/7 facilities.

We present a non-colinear sum frequency generation (NCSFG) technique that inherently incorporates temporal intensity shaping [1]. Our method is characterized by the mixing of two highly dispersed pulses (Fig. 1) which combine during sum-frequency generation to generate a pulse with a tailored temporal intensity profile. We expand on Raoult et al [19] of efficient narrowband second harmonic generation in thick crystals by adding third-order dispersion to simultaneously shape the output pulse. This method, which we call dispersion controlled nonlinear shaping (DCNS), can be broadly used to tailor pulses for the reduction of transverse emittance in photoinjector-based instrumentation.

* rlemons@slac.stanford.edu

ISBN: 978-3-95450-220-2 ISSN: 2673-5474 doi: 10.18429/JACoW-FEL2022-TUP10

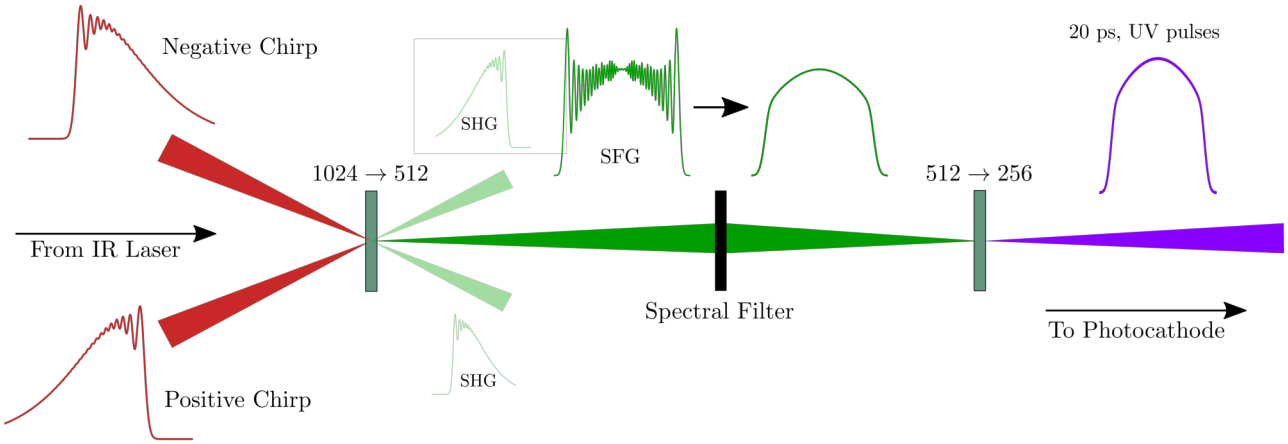

Figure 1: Schematic diagram of the DCNS method being used to generate a temporally flattened UV pulse from equal and oppositely dispersed infrared pulses. The spectral filter included between the two upconversion stages serves to eliminate unwanted oscillations on the edges of the optical pulse

EXPERIMENTAL IMPLEMENTATION

The electric field of a laser pulse in frequency space is given by $E(\omega) = A(\omega)e^{i\varphi(\omega)}$ where $A(\omega)$ is the spectral amplitude, typically modeled as a Gaussian distribution around the central frequency, and $\varphi(\omega)$ is the spectral phase. We define $\varphi(\omega)$ via a Taylor expansion about the central frequency,

$$\varphi(\omega) = \varphi_0 + \varphi_1(\omega - \omega_0) + \frac{\varphi_2}{2!}(\omega - \omega_0)^2 + \frac{\varphi_3}{3!}(\omega - \omega_0)^3 + \frac{\varphi_4}{4!}(\omega - \omega_0)^4 + \dots \quad (2)$$

where φ_j is the j^{th} derivative of $\varphi(\omega)$ evaluated at ω_0. Dropping the first two terms, which are arbitrary for our purposes, we focus on the next two terms, second order dispersion (SOD), φ_2, and third order dispersion (TOD), φ_3. SOD is a linear instantaneous temporal chirp on the pulse primarily affecting duration while TOD is a quadratic instantaneous chirp creating temporal oscillations on either the leading or falling edge of the pulse. Additionally, we define the ratio $\alpha = \varphi_3/\varphi_2$ (s) allowing us to set pulse duration with SOD and change shape with α.

Our laser system is driven by a Light Conversion Carbide 1024 nm, 40 μJ, 1 MHz, 246 fs commercial laser with an approximately 7 nm full width at half maximum (FWHM) spectral bandwidth. Based on these laser parameters we constructed a matched free-space grating-based optical compressor and stretcher set in an off-littrow configuration designed to impart ± 27.311 ps^2 SOD and ∓ 0.28 ps^3 TOD onto the IR pulses. SOD of this magnitude results in pulses with duration $\approx$ 300 ps however, it is necessary in order to achieve the proper TOD while maintaining efficiency and physically constructible designs. To correct this excessive SOD without changing TOD, we pass both beams through a chirped volume Bragg grating [20] designed to apply ∓ 24.75 ps^2 of SOD. This leaves the IR pulses with values of SOD and TOD of ± 2.5611 ps^2 and ∓ 0.28 ps^3 respectively which were chosen so that the FWHM of the laser pulse would be 25 ps in time [18] with an approximately flat temporal profile.

Once the spectral phase of the IR pulses was modified, they were used as the two input pulses to the NC-SFG setup. After passing through a 2 mm thick β-barium borate (BBO) crystal, the SFG pulses were passed through two spectral filters centered at 514 nm with a FWHM of 2 nm. The central wavelength of the spectral filters was angle tuned towards 512 nm with one being tuned farther such that the combined effective filter was centered at 512 nm but with a FWHM of $\approx$ 1nm. The filtered SFG pulses finally were used to generate the necessary UV pulses in a 1.5 mm BBO crystal and then sent to a difference frequency cross-correlator to measure temporal intensity.

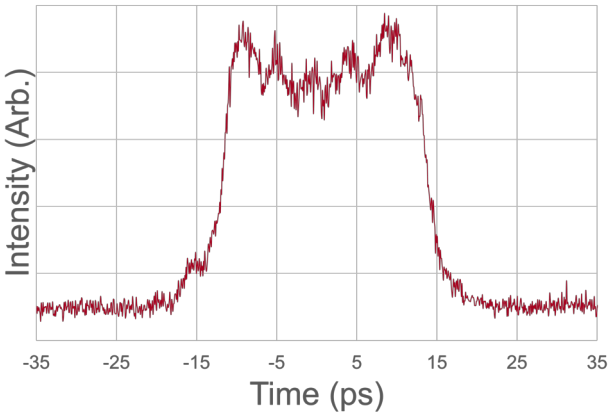

Figure 2: Experimental temporal intensity trace

The UV temporal intensity profile (Fig. 2) has a FWHM duration of 26 ps with 90:10 rise/fall times of 4 ps. The temporal intensity profile is characterized by a significantly longer and flatter peak intensity region than that of a Gaussian with a similar duration. However, there is also a significant oscillation across the plateau of the pulse. This oscillation is likely caused by excessive spectral filtering

ISBN: 978-3-95450-220-2 ISSN: 2673-5474 doi: 10.18429/JACoW-FEL2022-TUP10

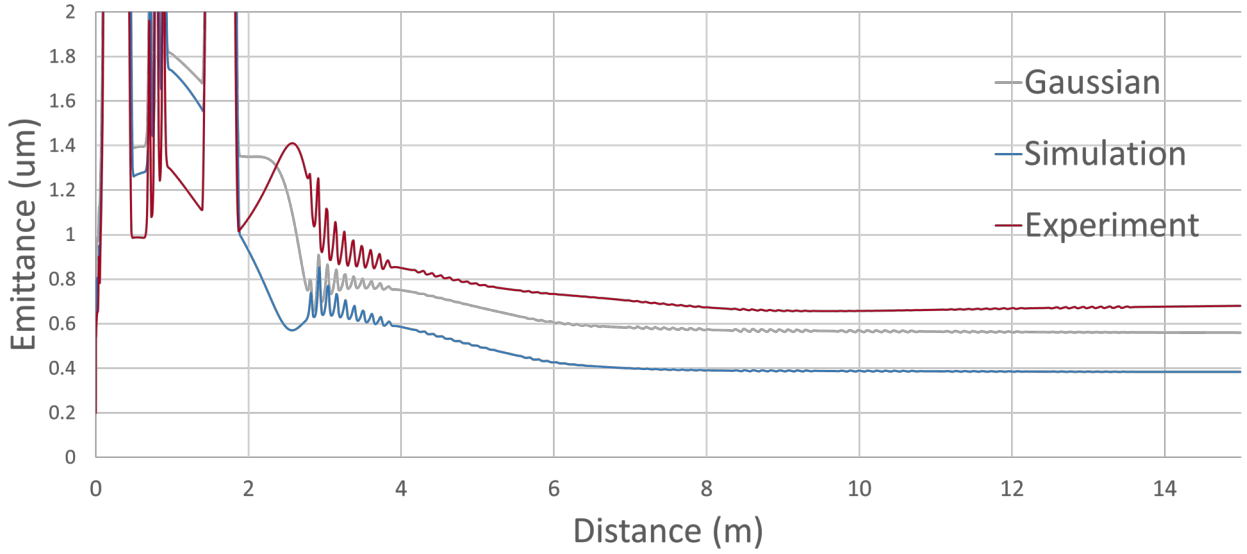

Figure 3: Transverse emittance of electron bunches generated from photo-excitation laser pulses with different temporal intensity profiles from the LCLS-II photocathode over the first 15 meters. The currently implemented Gaussian profile (gray) has a final emittance of 0.55 um while the experimental and simulation DCNS pulses achieve 0.38 um and 0.68 um respectively

in the UV generation crystal due to its thickness limiting the possible spectral acceptance bandwidth. Filtering due to this effect would overshadow the filtering achieved with the two spectral filters on the SFG beam but could be easily corrected by using a thinner BBO crystal.

To evaluate the possible electron generation performance, we simulate the photoinjector system and the first 15 meters of acceleration at LCLS-II. This serves to limit the simulation to a region where space-charge forces are not yet damped by highly relativistic speeds and the effect of the laser is prominent. The simulation code used for e-beam dynamics is OPAL [21], and for particle distribution generation [22]. While supplying the DCNS pulses is straightforward, determining the optimal FWHM and spot size on the cathode is not. The strength of the space charge forces is directly impacted by both the FWHM and spot size, which then impacts how strong the external forces need to be to limit emittance growth. To determine optimal laser and machine settings for an individual temporal profile, the simulation would need to be run in combination with an optimization algorithm such as NSGA-II [23]. In our case, the simulation was run with parameters optimal for the Gaussian distribution and is likely to overestimate the emittance of the other profiles.

Figure 3 displays the emittance of the electron bunches generated by the currently implemented Gaussian beam, the experimental DCNS pulse trace, and a simulated DCNS pulse with the same generation parameters. The simulation DCNS pulse also does not take into account the excessive filtering from the thick UV crystal. All temporal profiles initially have similar emittance values around 0.55 um immediately after the cathode. After the dispersive sections, noted by the sections with significant emittance increase, the emittance from the three profiles settles out to 0.55 um, 0.68 um, and 0. 38 um for the Gaussian, experimental, and simulation profiles respectively. As noted previously, the non-optimal parameters are likely to increase emittance for both the DCNS profiles compared to the Gaussian case, however, the temporal oscillations across the plateau of the experimental profile are the largest contributor to a larger emittance value, and the discrepancy compared to simulation. A temporal profile with reduced or eliminated oscillations is thus likely to exceed the emittance performance of the currently implemented Gaussian profile. This is supported by the simulated DCNS pulse maintaining a 30% decrease in emittance compared to the Gaussian profile and consistent with the results presented in Lemons et al. [1]. As such, the experimentally captured DCNS pulse still represents a significant step toward the implementation of a temporal pulse shaping technique that is compatible with the energies and repetition rates required by next-generation XFELs.

CONCLUSION

Electron emittance, and by extension the electron beam and x-ray beam brightness, can be improved through temporal tailoring of the photoinjector drive laser backing modern and next-generation XFELs. Available shaping methods for tailoring the excitation laser pulse are limited due to the required temporal duration, laser pulse energy, and repetition rate. We present the first experimental application of the DCNS method to generate tailored UV laser pulses capable of driving the LCLS-II photoinjector. We demonstrate the applicability of this method to the high pulse energy and high repetition rate regimes demanded by next-generation XFELs. The generated UV pulses with tailored temporal intensity

ISBN: 978-3-95450-220-2 ISSN: 2673-5474 doi: 10.18429/JACoW-FEL2022-TUP10

profiles are characterized by FWHM of 26 ps, sharp rise/fall time, and a region of extended and flattened peak intensity compared to the currently implemented Gaussian profile. Though the experimental DCNS pulses have temporal intensity oscillations across the plateau, and thus an increased emittance in simulation compared to Gaussian pulses, this is likely caused by a correctable experimental design choice. Electron bunches generated by simulated DCNS pulses using the same experimental parameters, without the conditions leading to the intensity oscillations, have upwards of 30% emittance decrease compared to the Gaussian profile. Our implementation of the DCNS method is a significant step toward realizing a system that can substantially extend the brightness of photoinjector systems worldwide without major configuration changes and thus enhance current scientific capabilities on existing accelerators and reduce the cost of future accelerator facilities.

ACKNOWLEDGEMENTS

We thank Yuantao Ding and Christopher Mayes at SLAC National Accelerator Laboratory for their helpful discussions.

This work is supported by the U.S. Department of Energy, Office of Science, Office of Basic Energy Sciences under Contract No. DE-AC02-76SF00515 and DE-SC0022559.

REFERENCES

[1] R. Lemons, N. Neveu, J. Duris, A. Marinelli, C. Durfee, and S. Carbajo, "Temporal shaping of narrow-band picosecond pulses via noncolinear sum-frequency mixing of dispersion-controlled pulses," *Physical Review Accelerators and Beams*, vol. 25, no. 1, p. 013 401, 2022.

[2] H. Wiedemann, "Particle beams and phase space," in *Particle Accelerator Physics*. 2015, pp. 213–251, doi:10.1007/978-3-319-18317-6_8

[3] Z. Huang and K.-J. Kim, "Review of x-ray free-electron laser theory," *Phys. Rev. ST Accel. Beams*, vol. 10, p. 034 801, 3 2007, doi:10.1103/PhysRevSTAB.10.034801

[4] Z. Huang *et al.*, "Suppression of microbunching instability in the linac coherent light source," *Physical Review Special Topics-Accelerators and Beams*, vol. 7, no. 7, p. 074 401, 2004.

[5] N. Liebster *et al.*, "Laguerre-gaussian and beamlet array as second generation laser heater profiles," *Physical Review Accelerators and Beams*, vol. 21, no. 9, p. 090 701, 2018.

[6] J. Tang *et al.*, "Laguerre-gaussian mode laser heater for microbunching instability suppression in free-electron lasers," *Physical Review Letters*, vol. 124, no. 13, p. 134 801, 2020.

[7] M. Krasilnikov *et al.*, "Experimentally minimized beam emittance from an l-band photoinjector," *Physical Review Special Topics-Accelerators and Beams*, vol. 15, no. 10, p. 100 701, 2012.

[8] O. Luiten, S. Van der Geer, M. De Loos, F. Kiewiet, and M. Van Der Wiel, "How to realize uniform three-dimensional ellipsoidal electron bunches," *Physical review letters*, vol. 93, no. 9, p. 094 802, 2004.

[9] S. Y. Mironov *et al.*, "Shaping of cylindrical and 3d ellipsoidal beams for electron photoinjector laser drivers," *Applied optics*, vol. 55, no. 7, pp. 1630–1635, 2016.

[10] Y. Li, S. Chemerisov, J. Lewellen, *et al.*, "Laser pulse shaping for generating uniform three-dimensional ellipsoidal electron beams," *Physical Review Special Topics-Accelerators and Beams*, vol. 12, no. 2, p. 020 702, 2009.

[11] M. D. Skeldon, "Optical pulse-shaping system based on an electro-optic modulator driven by an aperture-coupled-stripline electrical-waveform generator," *J. Opt. Soc. Am. B*, vol. 19, no. 10, pp. 2423–2426, 2002, doi:10.1364/JOSAB.19.002423

[12] J. Stohr, "Linac coherent light source ii (lcls-ii) conceptual design report," 2011, doi:10.2172/1029479

[13] S. Carbajo and K. Bauchert, "Power handling for lcos spatial light modulators," in *Laser Resonators, Microresonators, and Beam Control XX*, International Society for Optics and Photonics, vol. 10518, 2018, 105181R.

[14] M. Krasilnikov, Y. Chen, and F. Stephan, "Studies of space charge dominated electron photoemission at pitz," in *Journal of Physics: Conference Series*, IOP Publishing, vol. 1238, 2019, p. 012 064.

[15] S. Bettoni *et al.*, "Impact of laser stacking and photocathode materials on microbunching instability in photoinjectors," *Phys. Rev. Accel. Beams*, vol. 23, p. 024 401, 2 2020, doi:10.1103/PhysRevAccelBeams.23.024401

[16] C. Mitchell, P. Emma, J. Qiang, and M. Venturini, "Sensitivity of the microbunching instability to irregularities in cathode current in the lcls-ii beam delivery system," *proceedings NAPAC2016, Oct*, pp. 9–14, 2016.

[17] I. Will, H. I. Templin, S. Schreiber, and W. Sandner, "Photoinjector drive laser of the flash fel," *Optics Express*, vol. 19, no. 24, pp. 23 770–23 781, 2011.

[18] S. Gilevich *et al.*, "The lcls-ii photo-injector drive laser system," in *2020 Conference on Lasers and Electro-Optics (CLEO)*, IEEE, 2020, pp. 1–2.

[19] F. Raoult *et al.*, "Efficient generation of narrow-bandwidth picosecond pulses by frequency doubling of femtosecond chirped pulses," *Optics letters*, vol. 23, no. 14, pp. 1117–1119, 1998.

[20] S. Kaim, S. Mokhov, B. Y. Zeldovich, and L. B. Glebov, "Stretching and compressing of short laser pulses by chirped volume bragg gratings: Analytic and numerical modeling," *Optical Engineering*, vol. 53, no. 5, p. 051 509, 2013.

[21] A. Adelmann *et al.*, *Opal a versatile tool for charged particle accelerator simulations*, 2019.

[22] C. Gulliford, *DistGen: Particle distribution generator*, 2019, https://github.com/ColwynGulliford/distgen

[23] K. Deb, A. Pratap, S. Agarwal, and T. Meyarivan, "A fast and elitist multiobjective genetic algorithm: NSGA-II," *IEEE Trans. Evol. Comp.*, vol. 6, no. 2, pp. 182–197, 2002, doi:10.1109/4235.996017